


RESEARCH

Open Access



# SRSF1-mediated alternative splicing regulates bladder cancer progression and cisplatin sensitivity through HIF1A/BNIP3/mitophagy axis

Qikai Wu<sup>1,2†</sup>, Hao Yu<sup>1,2†</sup>, Huanyou Sun<sup>1,2†</sup>, Jiancheng Lv<sup>1,3†</sup>, Juntao Zhuang<sup>1,2</sup>, Lingkai Cai<sup>1,2</sup>, Lingjing Jiang<sup>1,2</sup>, Yuhang Chen<sup>1,2</sup>, Yiran Tao<sup>1,2</sup>, Kexin Bai<sup>1,2</sup>, Haiwei Yang<sup>1,2\*</sup>, Xiao Yang<sup>1\*</sup> and Qiang Lu<sup>1\*</sup> 

## Abstract

**Background** Alternative splicing (AS) is consistently linked to tumor progression. SRSF1, the first identified proto-oncogene in the serine/arginine-rich splicing factor (SRSF) protein family, plays a crucial role. However, the specific functions and potential mechanisms of SRSF1 in advancing bladder cancer (BCa) progression and influencing chemosensitivity remain largely unexplored.

**Methods** The expression of SRSF1 in BCa tissues and cell lines was investigated using quantitative real-time PCR (RT-qPCR) and western blotting. Survival analysis was employed to examine the association between SRSF1 expression and prognosis of BCa. The functions of SRSF1 were evaluated through proliferation assays, migration assays, IC50 determination assays, and tumorigenesis assays in nude mice. Subsequent RNA sequencing validated the relationship between SRSF1 alternative splicing and the mitophagy pathway. Mitochondrial membrane potential (MMP) was assessed using JC-1 staining. Mitophagy and autophagic flux were quantified using transmission electron microscopy and fluorescence imaging. RNA immunoprecipitation, CUT & RUN assays, and luciferase reporter assays were performed to validate the SRSF1/HIF1A/BNIP3 axis.

**Results** High expression of SRSF1 in BCa was significantly associated with poor prognosis. SRSF1 promoted the progression of BCa cells and conferred resistance to cisplatin both in vitro and in vivo. Mechanistically, SRSF1 interacted with pre-HIF1A via the RRM1/RRM2 domain, thereby enhancing the production of the transcription factor HIF1A through the alternative splicing pathway. This interaction subsequently activated the HIF1A/BNIP3 axis, which promoted mitophagy in BCa. Ultimately, this led to further progression of bladder cancer and a decrease in cisplatin sensitivity.

<sup>†</sup>Qikai Wu, Hao Yu, Huanyou Sun and Jiancheng Lv, have contributed equally.

\*Correspondence:

Haiwei Yang

haiweiyang@njmu.edu.cn

Xiao Yang

yangxiao2915@163.com

Qiang Lu

doctorlvqiang@njmu.edu.cn

Full list of author information is available at the end of the article



© The Author(s) 2025. **Open Access** This article is licensed under a Creative Commons Attribution-NonCommercial-NoDerivatives 4.0 International License, which permits any non-commercial use, sharing, distribution and reproduction in any medium or format, as long as you give appropriate credit to the original author(s) and the source, provide a link to the Creative Commons licence, and indicate if you modified the licensed material. You do not have permission under this licence to share adapted material derived from this article or parts of it. The images or other third party material in this article are included in the article's Creative Commons licence, unless indicated otherwise in a credit line to the material. If material is not included in the article's Creative Commons licence and your intended use is not permitted by statutory regulation or exceeds the permitted use, you will need to obtain permission directly from the copyright holder. To view a copy of this licence, visit <http://creativecommons.org/licenses/by-nc-nd/4.0/>.

**Conclusions** SRSF1 indicated poor prognosis and promoted the progression and cisplatin resistance of BCa cells through the HIF1A/BNIP3/mitophagy axis. It holds significant potential as a novel biomarker for the diagnosis and treatment of BCa, particularly in chemotherapy.

**Keywords** SRSF1, Bladder cancer, Alternative splicing, Mitophagy, Cisplatin resistance

## Introduction

Bladder cancer (BCa) is a commonly occurring malignant tumor of the urinary system, ranking ninth among all malignant tumors worldwide, posing a significant challenge due to its poor prognosis [1]. Systemic chemotherapy represents a crucial treatment modality for advanced or metastatic urothelial carcinoma [2]. Cisplatin-based neoadjuvant or adjuvant chemotherapy could improve the 5-year bladder cancer-specific survival [3]. Nevertheless, the overall response rate to chemotherapy remains low, at approximately 30–40% [4]. Consequently, this underscores the urgent need to explore new strategies to boost chemotherapy sensitivity in BCa.

Alternative splicing (AS) of pre-mRNA, influenced by splicing factors, affects over 95% of human genes, producing diverse proteins [5]. Among the five patterns mediated by these factors, skipped exon (SE), alternative 5' or 3' splice site selection (A5SS/A3SS), mutually exclusive exon (MXE), and intron retention (IR)-SE is the predominant form [6]. SE involves the splicing of exons along with flanking introns, leading to shorter protein isoforms. Recently, an increasing number of studies have demonstrated that SE is strongly linked to tumorigenesis and drug resistance [7].

SRSF1 (serine/arginine-rich splicing factor 1), characterized by two RNA recognition motifs (RRMs) and an RS domain, plays a role in RNA binding and protein interactions, respectively [8, 9]. Research has shown that SRSF1 can act as a pro-oncogene, involved in tumorigenesis and metastasis in lung cancer [10], liver cancer [11], and glioma [12]. For example, SRSF1 upregulation has been linked to breast cancer progression via the alternative splicing of PTPMT1 [13] and to gliomagenesis by affecting MYO1B pre-mRNA splicing [14]. Additionally, inhibiting SRSF1 has been shown to enhance gemcitabine-induced apoptosis in pancreatic ductal adenocarcinomas [15]. The potential involvement of SRSF1 in BCa splicing and its correlation with cisplatin resistance, however, remains to be elucidated.

Recent studies have revealed that mitophagy contributes to tumor progression. Mitophagy, a selective form of autophagy, is crucial for eliminating damaged or outdated mitochondria, thus preserving mitochondrial integrity and physiological functions [16]. This process is primarily orchestrated through two pathways: the ubiquitin-dependent and the ubiquitin-independent pathways [17].

The latter has been increasingly studied and involves key receptors such as NIX, BNIP3, and FUNDC1 that facilitate the direct encapsulation of mitochondria into autophagosomes by binding to LC3-II [18]. Notably, mitophagy has been identified as a survival mechanism in cancer cells. Studies indicate that suppressing mitophagy can enhance the efficacy of cancer treatments [19]. For example, cisplatin-induced mitophagy, which can be augmented by autophagy activators, has been observed in various studies including those by Zhao et al. [20]. Furthermore, Chen et al. [21] found that overexpressing galectin-1, thus promoting mitophagy, could increase cisplatin resistance in epithelial ovarian cancer cells. Conversely, genetic inhibition of key mitophagy mediators like BNIP3 [22], NIX [23], and FUNDC1 [24] has been shown to make cancer cells more vulnerable to chemotherapy. For instance, research has shown that while activating mitophagy can help shield neuroblastoma cells from cisplatin-induced apoptosis, inhibiting mitophagy leads to increased apoptosis [25]. These findings suggest that targeting mitophagy could be a promising strategy to enhance the sensitivity of BCa cells to cisplatin chemotherapy, potentially improving therapeutic outcomes.

In this study, we demonstrated that SRSF1 promoted the proliferation, migration, and cisplatin resistance of BCa cells both in vitro and in vivo assays. Additionally, SRSF1 enhanced BNIP3 production by promoting the alternative splicing of HIF1A, ultimately activating the mitophagy pathway. As a result, SRSF1 may serve as a viable biomarker and therapeutic target for the treatment of in BCa.

## Methods

### Human tissue specimens and cell lines

All 36 pairs of BCa tissues and adjacent normal tissues were acquired from BCa patients who underwent operation at the First Affiliated Hospital of Nanjing Medical University from 2017 to 2021. The tissues from BCa patients that were used in this study were approved by the Ethics Committee of The First Affiliated Hospital of Nanjing Medical University. All patients signed the informed consent and the study methodologies conformed to the standards set by the Declaration of Helsinki. The BCa cell lines (T24, RT4, 5637, BIU87, UMUC3, 253J, and J82) and urothelial cell line (SV-HUC-1) were acquired

through the Type Culture Collection of the Chinese Academy of Sciences (Shanghai, China).

### Cell culture and transfection

T24, UMUC3, and HEK 293T cells were cultured with Dulbecco's modified eagle's medium (DMEM) (Gibco, USA) containing 10% fetal bovine serum (FBS) (BI, Israel) in a 37 °C incubator with 5% CO<sub>2</sub>.

SRSF1 knockdown and overexpression lentivirus vectors were obtained from HANBIO (HANBIO, China). At 50 or 60% confluence in six-well plates, T24 or UMUC3 cells were transfected with SRSF1 overexpression lentivirus (SRSF1), negative control (vector), SRSF1 knockdown lentivirus (sh-SRSF1-1 and sh-SRSF1-2), and negative control (sh-NC). The transfected cells were selected using puromycin (4 and 8 µg/mL) on two occasions. Small interfering RNAs (siRNAs) targeting HIF1A and BNIP3 were obtained from GenePharma (Shanghai, China). Wild-type and mutant-type dual-luciferase reporter plasmids of BNIP3 were synthesized by TsingKe (Nanjing, China). Plasmids expressing FLAG-tagged wild-type SRSF1 (SRSF1-wt) and SRSF1 domain deletion mutants (SRSF1- $\Delta$ RRM1, - $\Delta$ RRM2, - $\Delta$ RS) were constructed using the pCDNA3.0-HA vector (HANBIO, China). The mito-Keima plasmid was synthesized by Genechem (Shanghai, China). T24 and UMUC3 cells were transfected with the mentioned plasmids and siRNAs using the Lipofectamine 3000 kit (Invitrogen, USA), following the provided guidelines. The siRNAs/shRNAs used in this research were listed in Supplementary Table S1.

### RNA isolation and quantitative real-time PCR (RT-qPCR)

Total RNA was extracted from cultured BCa cells and human tissues using Trizol Reagent (Invitrogen, USA). RNA was reverse transcribed into cDNA using HiScript II (Vazyme, China). RT-qPCR assays were conducted using the StepOne Plus Real-Time PCR System (Applied Biosystems, USA).  $\beta$ -actin served as the internal control. Primers were obtained from TsingKe (Nanjing, China) and are listed in Supplementary Table S2.

### Protein extraction and western blotting

Protein was extracted from cultured BCa cells and human tissues using RIPA lysis buffer containing protease inhibitors (Sigma, USA) and quantified using a bicinchoninic acid (BCA) assay kit (Beyotime, China). Proteins were separated using 10% SDS-PAGE and transferred onto polyvinylidene fluoride (PVDF) membranes (Millipore, USA). PVDF membranes were blocked with 5% skim milk and incubated overnight at 4 °C with primary antibodies against SRSF1 (1:1000, Invitrogen, USA), HIF1A (1:1000, Proteintech, China), BNIP3 (1:5000, Proteintech, China), Beclin-1 (1:2000, Proteintech, China),

P62 (1:1000, Proteintech, China), LC3A/B (1:1000, CST, USA), NIX (1:1000, Proteintech, China), FUNDC1 (1:5000, Proteintech, China), PINK1 (1:1000, Proteintech, China), PARKIN (1:2000, Proteintech, China), FLAG (1:1000, CST, USA), or anti- $\beta$ -tubulin (1:1000, Origene, USA). Membranes were then washed and incubated with secondary antibody (1:5000, FDBio, China). Protein levels were detected using chemiluminescence (Bio-Rad, USA) and analyzed with Image Lab Software.

### Cell proliferation assay, cloning formation assay and EdU assay

For the cell proliferation assay, transfected cells were seeded into 96-well plates at densities of 1,000 T24 cells and 1,500 UMUC3 cells per well. Cell viability was assessed every 24 h (24, 48, 72, and 96 h) using the Cell Counting Kit-8 (CCK-8, Dojindo, Japan). Absorbance at 450 nm was measured using a microplate reader (Tecan, Switzerland).

For the colony formation assay, 800 T24 cells or 1,000 UMUC3 cells were seeded in six-well plates. After two weeks, cell colonies were fixed and consecutively stained with 4% paraformaldehyde and 0.1% crystal violet. Cell colonies were quantified using ImageJ software.

For the EdU assay, approximately  $2 \times 10^4$  T24 or UMUC3 cells were seeded in 12-well plates. After 24 h, the EdU assay (Beyotime, China) was performed according to the manufacturer's instructions.

### Scratch wound healing and transwell assay

In the scratch wound healing assay, when T24 or UMUC3 cells reached 90–100% confluence in six-well plates, monolayer cells were scraped using a 200 µl pipette tip and subsequently cultured in serum-free medium. After 24 h, images of BCa cells were captured using an Olympus microscope (Japan).

In the transwell migration assay,  $2 \times 10^4$  T24 cells or  $3 \times 10^4$  UMUC3 cells were seeded in the upper chamber containing serum-free medium, and a medium with 20% FBS was added to the lower chamber (Corning, USA). BCa cells in the upper chambers were fixed and sequentially stained with 4% paraformaldehyde and 0.5% crystal violet. Observations were made and documented using an Olympus microscope.

### IC50 determination

Transfected T24 and UMUC3 BCa cells were collected and seeded in a 96-well plate at densities of 5,000 and 4,000 cells per well, respectively. After overnight incubation, various concentrations of cisplatin (128, 64, 32, 16, 8, 4, and 2 µmol/L; TCI, Japan) were administered to the cells for a duration of 36 h. Cell viability was then assessed using the Cell Counting Kit-8 (CCK-8, Vazyme,

China) following standard protocols. IC<sub>50</sub> values were calculated using SPSS software. The suppression rate of cisplatin was calculated as  $1 - (\text{OD value of } x \mu\text{M} / \text{OD value of } 0 \mu\text{M}) * 100\%$ .

#### Detection of mitochondrial membrane potential(MMP)

Mitochondrial membrane potential was assessed using JC-1 staining (Beyotime, China), with observations made using confocal microscopy (Leica, Germany).

#### Immunofluorescence

T24 and UMUC3 cells were transfected with mRFP-GFP-LC3 adenovirus (KEYGEN BIOTECH CORP, LTD, China) as per the manufacturer's instructions. At 24 h post-transfection, cells were treated with either CCCP (10  $\mu\text{mol/L}$ , Beyotime, China) or cisplatin (4  $\mu\text{mol/L}$ ) for an additional 24 h. Cells were then stained with MitoTracker Red (Beyotime, China) for the MitoTracker Red assay. Subsequently, cells were imaged using a confocal microscope (Leica, Germany). Mitophagosomes were identified by the merging of yellow spots from RFP and GFP puncta. For BNIP3 colocalization studies, treated cells were fixed with 4% paraformaldehyde for 30 min, washed with PBS, permeabilized with Triton X-100 (Beyotime, China), and blocked with QuickBlock (Beyotime, China) each for 30 min. Cells were incubated overnight at 4 °C with primary antibodies (BNIP3 1:5000, Proteintech, China) followed by a 1-h incubation with secondary antibodies (CoraLite 647-conjugated AffiniPure goat anti-mouse IgG (H+L), 37 °C). Further imaging was conducted using confocal microscopy (Leica, Germany) to collect visual data.

#### Transmission Electron Microscopy (TEM)

T24 and UMUC3 cells were fixed with ice-cold glutaraldehyde (Servicebio, China), followed by processing in the Core Facility (Servicebio, China). Specimens were examined using a JEOL JEM-2100 transmission electron microscope.

#### RNA immunoprecipitation assay (RIP)

Cells were lysed using RIPA buffer, and RNA immunoprecipitation was performed using the Magna RIP Kit (Millipore, USA) according to the manufacturer's instructions. RNA precipitation utilized antibodies specific to SRSF1 (Invitrogen, USA), FLAG (CST, USA), and control immunoglobulin G (IgG) (Millipore, USA). Input and coimmunoprecipitated RNAs were extracted using TRIzol reagent (Invitrogen, USA) for RT-qPCR analysis.

#### Dual-luciferase reporter assay

293 T cells were transfected with plasmids containing either wild-type or mutant BNIP3 promoter fragments,

and siRNA of HIF1A using Lipofectamine 3000 (Invitrogen, USA). After 24 h, luciferase activity was determined using the Dual Luciferase Assay Kit (GeneCopoeia, China).

#### CUT & RUN for qPCR

We performed the CUT & RUN assay using the Hyperactive CUT & RUN Assay Kit (Vazyme, China), adhering to the manufacturer's guidelines. Briefly, BCa cells underwent 24-h hypoxia exposure prior to analysis. Cells were collected and incubated with activated ConA Beads Pro at room temperature for 10 min, and subsequently incubated overnight with antibodies against either HIF-1A (Proteintech, USA) or IgG (Millipore, USA). After washing, cells were co-incubated with pA/G-Tnp Pro for 60 min, followed by DNA Extract Beads Pro for 20 min to release DNA fragments. Primers used for qPCR in the CUT & RUN assay are detailed in Supplementary Table S2.

#### Xenograft experiments in nude mice

A total of  $5 \times 10^6$  T24 cells transfected with sh-SRSF1 or corresponding negative control were subcutaneously injected into the axilla of BALB/C nude mice (4 weeks old, female). Mice in the experimental group received a 2.5 mg/kg dose of cisplatin intraperitoneally every three days for one week post-inoculation, while those in the control group were administered normal saline. Tumor volume (V) was calculated weekly using the formula  $V = (W^2 \times L) / 2$ , where W is width and L is length, measured using calipers. After four weeks, all nude mice were euthanized, and tumor samples were excised for further analysis. Ethical approval for the animal experiments was obtained from the Animal Ethics Committee at Nanjing Medical University.

#### Immunohistochemistry

Paraffin-embedded tumors derived from female nude mice were sectioned into 4- $\mu\text{m}$  slices and mounted onto slides. The sections were rehydrated through a series of ethanol solutions of varying concentrations. Antigen retrieval was conducted via microwave heating. The slides were then incubated in 3% hydrogen peroxide for 10 min to quench endogenous peroxidase activity. Subsequently, the sections were incubated with primary antibodies targeting SRSF1 (1:500, Abcam, USA) and BNIP3 (1:500, Protech, China) at 4 °C overnight. The following day, the slides were incubated with an HRP-conjugated secondary antibody (1:5000, Abcam, USA) at room temperature for 30 min. Microscopic examination was employed to capture and document the resultant staining.



## Statistical analysis

Data were analyzed utilizing GraphPad Prism version 8.0 (GraphPad Software, Inc., La Jolla, CA) and SPSS version 22.0 (IBM Corp., Armonk, NY, USA). The results were presented as mean  $\pm$  standard deviation (SD). Differences between groups were assessed using Student's t-test and one-way ANOVA. Overall survival (OS) rates were calculated using the Kaplan–Meier method. Statistical significance was established at *P* values less than 0.05.

## Results

### SRSF1 was upregulated in BCa tissues, cell lines and associated with poor prognosis

Pan-cancer analysis demonstrated that SRSF1 was highly expressed in 15 tumor types, including bladder cancer (BLCA), when compared to normal tissues (Fig. 1A). Utilizing the BEST database (<https://rookieutopia.hip-plot.com.cn/>), we explored the expression and prognostic implications of SRSF1 in bladder cancer. GSE154261 data revealed that elevated SRSF1 expression was strongly correlated with poor prognosis (Fig. 1B). Analysis of TCGA-BLCA data showed that SRSF1 levels were significantly higher in BCa tissues than in normal tissues and positively associated with advanced pathological grades in BCa patients (Fig. 1C–D). Data from GSE37815 indicated that high SRSF1 expression correlated with an increased recurrence rate (Fig. 1E). Moreover, high SRSF1 expression was linked to reduced sensitivity to cisplatin in BCa patients, as per IMvigor 210 data (Fig. 1F). We analyzed 36 pairs of BCa and adjacent normal tissues, confirming higher SRSF1 expression at both RNA (Fig. 1G) and protein levels (Fig. 1H) in BCa tissues. Additionally, SRSF1 expression was significantly elevated in seven BCa cell lines compared to SV-HUC-1 cells (Fig. 1I–J). There was a positive correlation between SRSF1 expression and both the stage and grade of the tumor in BCa patients (Table 1). Kaplan–Meier analysis indicated that patients with higher SRSF1 expression had poorer overall survival (Fig. 1K). Therefore, we speculated that SRSF1 may act as stimulator in BCa.

### SRSF1 promoted the progression and cisplatin-resistance of BCa cells in vitro and in vivo

To elucidate the role of SRSF1 in BCa, we employed SRSF1 overexpression and knockdown lentiviruses in T24 and UMUC3 cells, with the transfection efficiency confirmed by RT-qPCR and western blotting (Fig. 2A–B). SRSF1 knockdown in T24 cells was found to inhibit proliferation as evidenced by the CCK8 assay (Fig. 2C), colony formation assay (Fig. 2D), and EdU assay (Fig. 2E). Conversely, overexpression of SRSF1 in UMUC3 cells demonstrated the opposite effect. In scratch wound healing and transwell migration assays, SRSF1 promoted the migratory capabilities of T24 and UMUC3 cells (Fig. S1). To evaluate the impact of SRSF1 on cisplatin sensitivity, CCK-8 assays revealed decreased cell viability with increasing cisplatin concentrations. Interestingly, SRSF1 knockdown enhanced the inhibitory effect of cisplatin, evidenced by a significant drop in IC50 values, indicating increased drug sensitivity (Fig. 2F). Conversely, SRSF1 overexpression reduced cisplatin sensitivity (Fig. 2G). In vivo experiments involving subcutaneous injection of SRSF1 knockdown T24 cells into nude mice demonstrated reduced tumor growth when compared to controls (Fig. 2H). Additionally, treatment with cisplatin resulted in significantly smaller tumor volumes and weights, especially in the SRSF1 knockdown group treated with cisplatin (Fig. 2I–J). Thus, the in vivo data confirmed that SRSF1 knockdown not only impeded tumor proliferation but also enhanced the therapeutic efficacy of cisplatin in treating BCa.

### SRSF1 may promote BCa cells progression and cisplatin-resistance through mitophagy pathway

RNA sequencing analysis was conducted on three pairs of SRSF1 knockdown and corresponding control T24 cells. This was followed by the Kyoto Encyclopedia of Genes and Genomes (KEGG) analyses to elucidate the pathways and genes influenced by the altered expression of SRSF1. The results revealed significant enrichment of the mitophagy pathway upon knockdown of SRSF1 (Fig. 3A). Analysis of the volcano plot

(See figure on next page.)

**Fig. 1** SRSF1 was upregulated in BCa tissues, cell lines and associated with poor prognosis. **A** The expression of SRSF1 in TCGA pan-cancers and relative normal tissues (\**P* < 0.05, \*\**P* < 0.01, \*\*\**P* < 0.001, Student's t-test). **B** The high expression of SRSF1 was highly associated with worse prognosis in GSE154261 data. **C–D** TCGA-BLCA data indicated that SRSF1 was highly expressed in bladder cancer compared with normal tissues and positively correlated with higher pathological grades in BCa patients. **E–F** GSE37815 data indicated that high expression of SRSF1 was associated with a higher recurrence rate, and patients with high SRSF1 expression exhibited reduced sensitivity to cisplatin in the IMvigor 210 data. **G** The expression of SRSF1 in 36 pairs of BCa tissues was validated by RT-qPCR (\*\*\**P* < 0.001, Student's t-test). **H** The expression of SRSF1 in 8 pairs of BCa tissues was validated by western blotting. **I–J** The expression of SRSF1 in seven BCa cell lines and SV-HUC cell line was confirmed by RT-qPCR and western blotting (\*\*\**P* < 0.001, Student's t-test). **K** The correlation between SRSF1 and overall survival in BCa patients was confirmed through Kaplan–Meier analysis (The average RNA expression value of SRSF1 in 36 patient tissues using RT-qPCR was calculated, with samples above the average classified as "high SRSF1 expression" and those below the average classified as "low SRSF1 expression.")

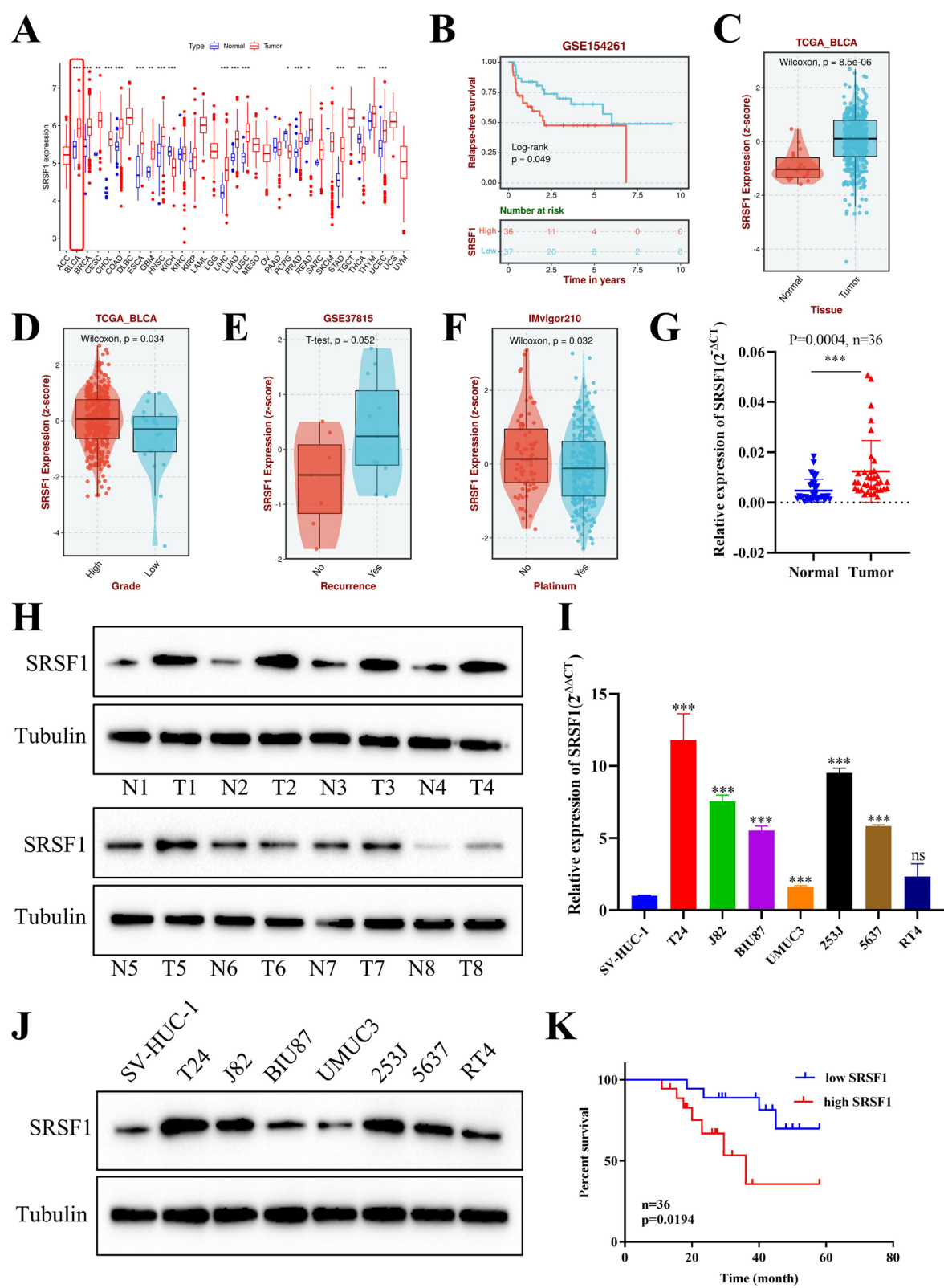


**Fig. 1** (See legend on previous page.)

**Table 1** Associations between the expression level of SRSF1 and clinicopathological features in BCa patients

Characteristics	Case	SRSF1		P value
		Low	High	
All cases	36	12	24	
Age (years)				0.473
<65	15	4	11	
≥65	21	8	13	
Gender				0.777
Female	8	3	5	
Male	28	9	19	
TNM stage				<b>0.007</b>
pTa-pT1	13	8	5	
pT2-pT4	23	4	19	
Histological grade				<b>0.013</b>
Low	14	9	5	
High	22	5	17	
Tumor Size (cm)				0.236
<3	16	7	9	
≥3	20	5	15	
Lymph metastasis				0.102
No	9	5	4	
Yes	27	7	20	

Bold values often represent data points that meet predefined thresholds for statistical significance (e.g.,  $P < 0.05$ )

and heatmap indicated a substantial downregulation of genes associated with the mitophagy pathway in the SRSF1 knockdown group (Fig. 3B–C), suggesting that the change of SRSF1 in BCa cells may affect the mitophagy pathway. In SRSF1 knockdown BCa cells, a decrease was observed in Beclin-1 and the LC3B II/LC3B I ratio, while an increase in p62 was noted, underscoring the positive regulatory role of SRSF1 in the autophagy pathway. In contrast, in SRSF1 overexpression cells, the expression levels of these markers demonstrated the opposite trend (Fig. 3D). The green fluorescence of shRNA compromises subsequent experimental observations; consequently, small interfering RNA of SRSF1 was selected for partial experimental.

RNA interference efficacy was confirmed through RT-qPCR and western blotting analysis of SRSF1 knockdown (si-SRSF1) (Fig. S2A–B), with si-SRSF1-2 identified as the most effective siRNA for further studies. Mitochondrial membrane potential (MMP) was assessed using JC-1 dye uptake, revealing an increase in MMP in the SRSF1 knockdown cells compared to the control (si-NC) group (Fig. 3E–F). We employed the commonly used mitophagy agonist, CCCP, to facilitate clearer observations. Results indicated a decrease in MMP, promoting mitophagy in BCa cells. Furthermore, after co-culturing with cisplatin, we observed that cisplatin could also reduce the MMP in BCa cells, thereby enhancing mitophagy (Fig. 3E–F). Further transfection with the mito-Keima plasmid in SRSF1 knockdown cell lines confirmed a reduction in mitophagy following SRSF1 knockdown (Fig. S2C–D). Moreover, the colocalization of mitochondria with autophagosomes, evidenced through merged fluorescence imaging of MitoTracker and GFP-LC3 markers, was significantly decreased in SRSF1 knockdown cells, but enhanced upon treatment with CCCP and cisplatin in T24 and UMUC3 cells, respectively (Fig. 3G–H). These findings preliminarily suggested that SRSF1-dependent regulation of the mitophagy pathway may play an active role in modulating the progression and cisplatin resistance in BCa.

#### SRSF1 affected BNIP3 mediated mitophagy in BCa cells

To investigate the role of SRSF1 in mitophagy in BCa cells, transmission electron microscopy (TEM) was used to observe mitochondrial structures. After knocking down SRSF1, there was a notable decrease in the number of mitophagosomes (Figs. 4A, S3A–B). Conversely, treatment with CCCP or cisplatin for 36 h may lead to a significant production in mitophagosomes in T24 and UMUC3 cells (Figs. 4A, S3A–B). We further examined the expression of key mitophagy-related proteins in BCa cells with either overexpressed or knocked down SRSF1. The findings demonstrated that BNIP3 expression decreased significantly following the knockdown of SRSF1, whereas the levels of PINK1, Parkin, NIX, and

(See figure on next page.)

**Fig. 2** SRSF1 promoted the progression and cisplatin-resistance of BCa cells in vitro and in vivo. **A–B** SRSF1 knockdown and overexpression efficiency in T24 and UMUC3 cells was confirmed by RT-qPCR and western blotting. ( $***P < 0.001$ , Student's t-test). **C–E** SRSF1 knockdown could inhibit the proliferation while SRSF1 overexpression could promote the proliferation of T24 and UMUC3 cells through CCK8 assay, colony formation assay, and EdU assay ( $*P < 0.05$ ,  $**P < 0.01$ ,  $***P < 0.001$ , Student's t-test). **F–G** Knockdown of SRSF1 expression increased the suppression rate of cisplatin and decreased IC50 to cisplatin in T24 cells by CCK8 assays. SRSF1 overexpression decreased the suppression rate of cisplatin and increased IC50 to cisplatin in UMUC3 cells by CCK8 assays ( $*P < 0.05$ ,  $**P < 0.01$ ,  $***P < 0.001$ , Student's t-test). **H** Picture of the nude mice xenograft tumor model with SRSF1 knockdown or negative control T24 cells, which injected with cisplatin or normal saline. **I** Nude mice tumor volumes were measured weekly in four groups ( $**P < 0.01$ ,  $***P < 0.001$ , Student's t-test). **J** Tumor weights of the four groups were measured after tumors were dissected ( $*P < 0.05$ ,  $**P < 0.01$ ,  $***P < 0.001$ , Student's t-test)

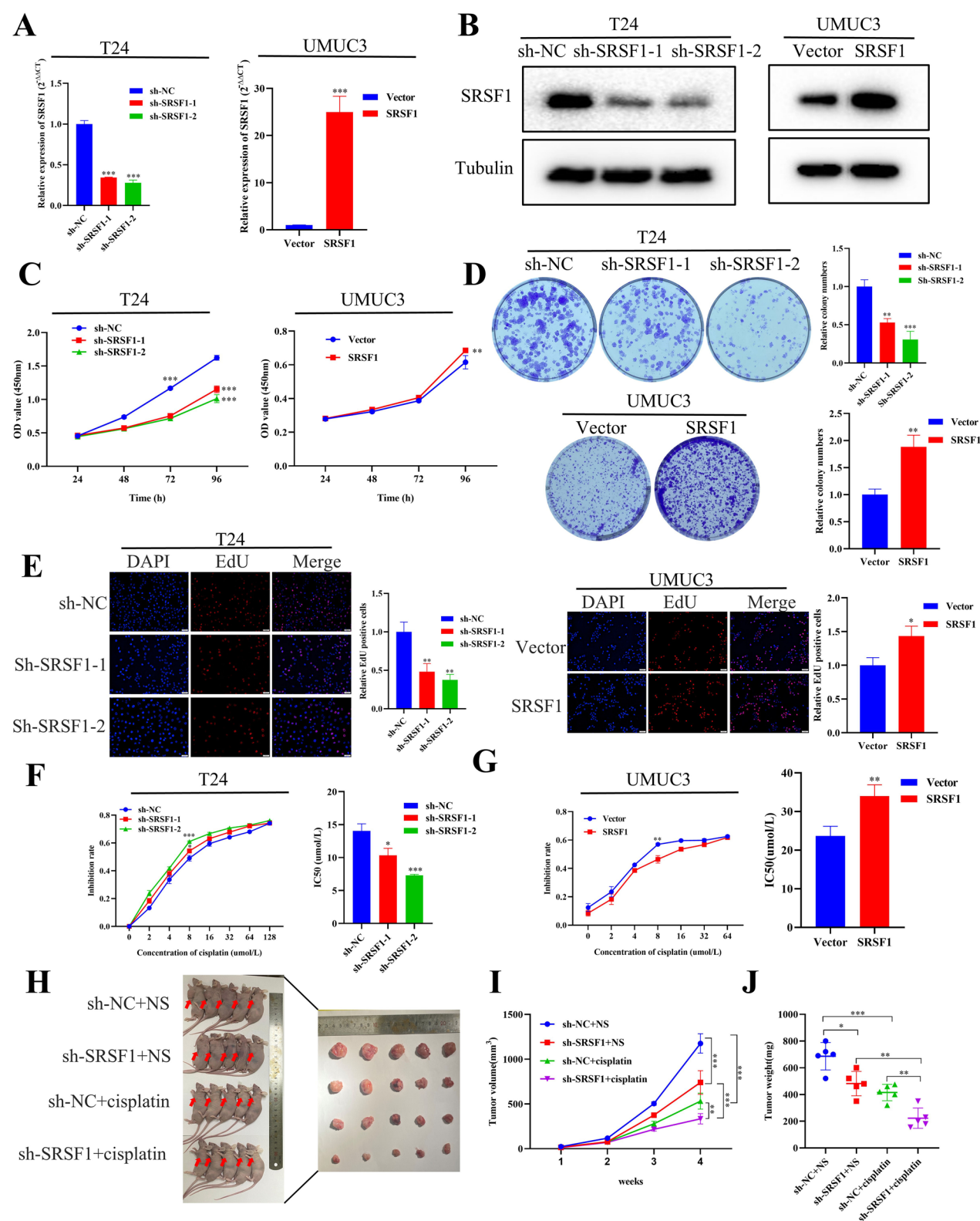


**Fig. 2** (See legend on previous page.)



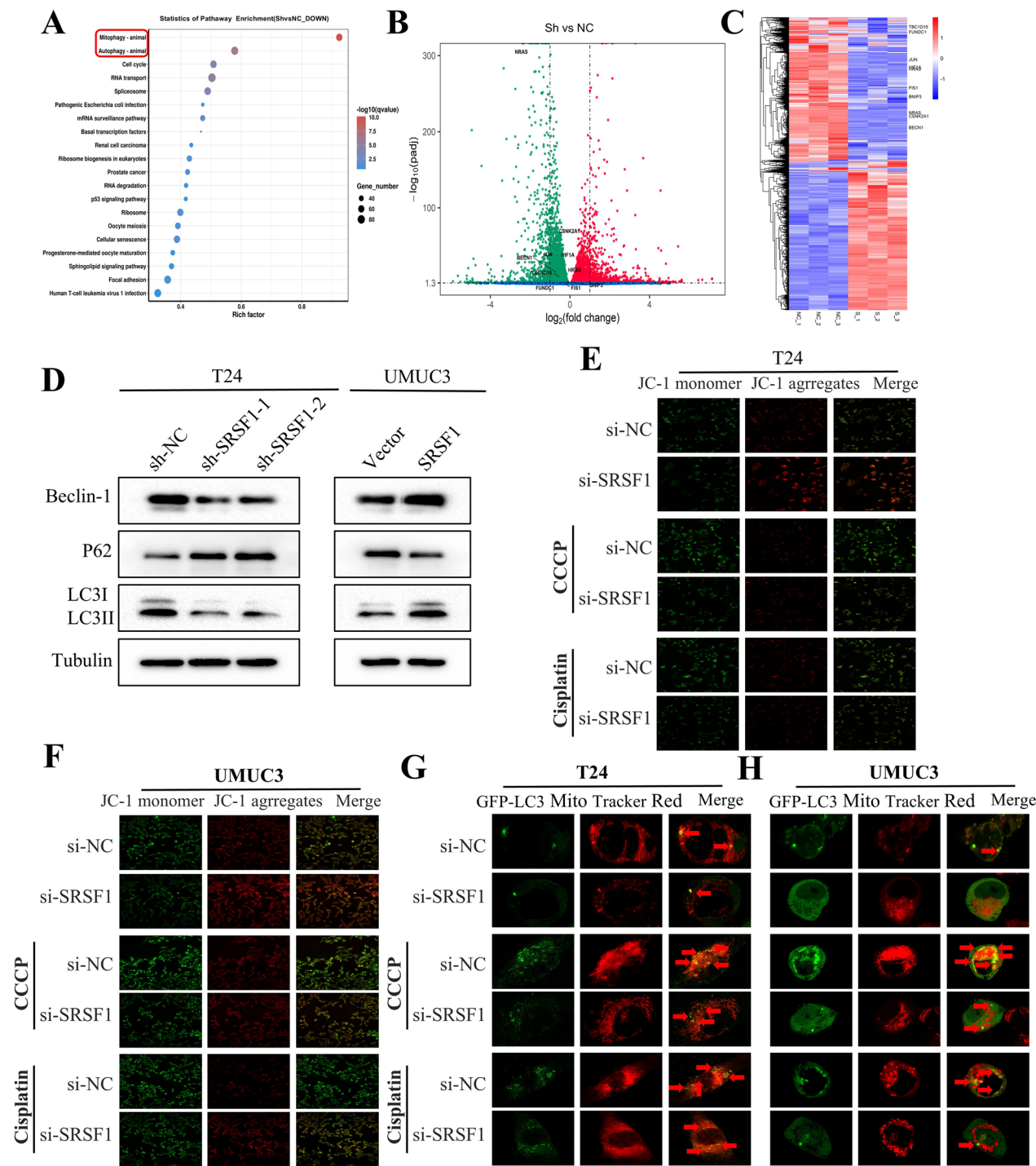


**Fig. 3** SRSF1 may promote BCa cells progression and cisplatin-resistance through mitophagy pathway. **A** KEGG analysis of RNA sequencing. **B** Volcano plot of RNA sequencing that indicated the differentially expressed genes in mitophagy pathway, including HIF1A and BNIP3. **C** Heat map of RNA sequencing in three pairs of SRSF1 knockdown and relative control T24 cells. **D** Western blotting analysis of autophagy-related proteins in T24 and UMUC3 cells with SRSF1 knockdown or overexpression. **E–F** After treatment with cisplatin or CCCP, mitochondrial damage levels in SRSF1 knockdown or relative control BCa cells were assessed using the mitochondrial membrane potential detection kit (JC-1). When the mitochondrial membrane potential (MMP) is low, JC-1 exists in monomer form and cannot aggregate in the mitochondria in the matrix, which produces green fluorescence. When the MMP is high, JC-1 aggregates in the mitochondrial matrix to form polymers and produces red fluorescence. **G–H** The colocalization of mitochondria and autophagosomes was determined by staining with MitoTracker Red. In brief, after transfection with mRFP-GFP-LC3 adenovirus for 24 h, SRSF1 was transfected with small interference for 24 h and then stained with MitoTracker Red for 30 min before observation

FUNDC1 remained relatively unchanged. Conversely, with SRSF1 overexpression, there was a marked increase in BNIP3 expression (Fig. 4B). Subsequent analysis targeted the top ten genes implicated in the mitophagy pathway (NRAS, BECN1, JUN, CSNK2A1, FUNDC1, TBC1D15, FIS1, HIF1A, HRAS, BNIP3), revealing that BNIP3 exhibited considerable expression changes following SRSF1 modulation (Fig. S2E–F). RT-qPCR analysis confirmed that the downregulation of SRSF1 resulted in decreased BNIP3 expression, whereas its upregulation led to increased BNIP3 expression (Fig. 4C). TCGA-BLCA data analysis confirmed a positive correlation between SRSF1 and BNIP3 expression levels (Fig. 4D). BNIP3 was found to be highly expressed in BCa tissues compared to adjacent normal tissues (Fig. 4E), and Pearson's correlation analysis further supported a positive relationship between BNIP3 and SRSF1 expression (Fig. 4F). Immunohistochemistry experiments further demonstrated that BNIP3 levels positively correlated with SRSF1 levels (Fig. 4G). Additionally, BNIP3 expression was significantly elevated in BCa tissues compared to normal tissues through western blotting experiments (Fig. S3C).

#### BNIP3 promoted the proliferation, migration, and cisplatin-resistance of BCa cells in vitro

To elucidate the functional impact of BNIP3, small interference RNA targeting BNIP3 (si-BNIP3) or control siRNA (si-NC) were transfected into T24 and UMUC3 BCa cells. The efficiency of transfection was confirmed by RT-qPCR and western blotting (Fig. S4A–B). BNIP3 was observed to promote the proliferation of T24 and UMUC3 cells, as evidenced by CCK-8 assays (Fig. S4C) and colony formation assays (Fig. S4D). Additionally, EdU assays indicated enhanced cellular proliferation mediated by BNIP3 (Fig. S4E–F). In scratch wound healing assays and transwell assays, a decrease in migratory rate was apparent in cells with knocking down BNIP3 (Fig. S4G–J). Crucially, BNIP3 knockdown led to a significant increase in the inhibitory effect of cisplatin as well

as a decrease in IC<sub>50</sub> values, indicating heightened sensitivity to cisplatin (Fig. 4H–I).

#### SRSF1 regulated the splicing of HIF1A in BCa cells

RNA sequencing disclosed significant impacts on AS in BCa cells following alterations in SRSF1 expression. Despite SRSF1 being a classical splicing factor, its specific roles and the implicated splicing pathways in BCa cells remained unclear. To investigate, we analyzed differential AS events from the RNA sequencing data, which revealed that SE was the predominant AS event, accounting for 64.19% following SRSF1 knockdown (Fig. 5A). Initial studies focused on the potential regulation of BNIP3 splicing by SRSF1. However, no significant changes were observed. RIP assays demonstrated that the anti-SRSF1 antibody did not enrich BNIP3 pre-mRNA compared to the anti-IgG antibody in BCa cells (Fig. 5B). Reverse transcriptase PCR (RT-PCR) supported these findings, showing no contribution of SRSF1 to BNIP3 isoform production (Fig. 5C). Subsequently, our attention shifted to HIF1A within the mitophagy pathway, situated directly upstream of BNIP3 (Fig. S5A). We hypothesized that SRSF1 may indirectly influence BNIP3 production by modulating HIF1A splicing. RIP assays validated this hypothesis, confirming the binding of SRSF1 to HIF1A pre-mRNA (Fig. 5D). Analysis of TCGA-BLCA data portrayed a positive correlation between SRSF1 and HIF1A expression levels (Fig. 5E). HIF1A expression was significantly upregulated in BCa tissues compared to adjacent normal tissues (Fig. 5F), and Pearson's correlation analysis further confirmed a positive relationship between HIF1A and SRSF1 expression (Fig. 5G). To further investigate SRSF1-influenced AS, various HIF1A transcripts were evaluated. Among the 15 exons in the human HIF1A gene, exon 14 regulation by AS enables the generation of two distinct transcript variants (Fig. S5B). RT-PCR, using specific primers targeting all exon-skipping or exon-including isoforms, disclosed significant induction of exon 14 skipping, facilitating the expression of a truncated HIF1A isoform in SRSF1 knockdown cells (Fig. 5H–I). To characterize the interaction region between SRSF1 and HIF1A, plasmids

(See figure on next page.)

**Fig. 4** SRSF1 affected BNIP3 mediated mitophagy in BCa cells. **A** Representative TEM images of mitophagosomes (red arrow) were shown in SRSF1 knockdown and relative control. Scale bars indicate 2, 5  $\mu$ m CCCP or cisplatin increased the production of mitophagosomes in T24 and UMUC3 cells. **B** Western blotting was used to verify the key proteins involved in two pathways in mitophagy. **C** RT-qPCR assay demonstrated downstream target BNIP3 in the mitophagy pathway was positively altered with SRSF1 knockdown or overexpression (\*\* $P < 0.01$ , \*\*\* $P < 0.001$ , Student's t-test). **D** Correlation analysis confirmed a positive association between SRSF1 and BNIP3 in the TCGA-BLCA cohort. **E** The expression of BNIP3 in BCa tissues was validated by RT-qPCR (\* $P < 0.05$ , Student's t-test). **F** Pearson's correlation analysis was applied to confirm the correlation of SRSF1 and BNIP3. **G** The expression of BNIP3 in xenograft tumors is consistent with the expression of SRSF1 by immunohistochemistry. **H–I** Knockdown of BNIP3 expression increased the suppression rate of cisplatin and decreased IC<sub>50</sub> to cisplatin in T24 and UMUC3 cells by CCK8 assays (\* $P < 0.05$ , \*\* $P < 0.01$ , \*\*\* $P < 0.001$ , Student's t-test)

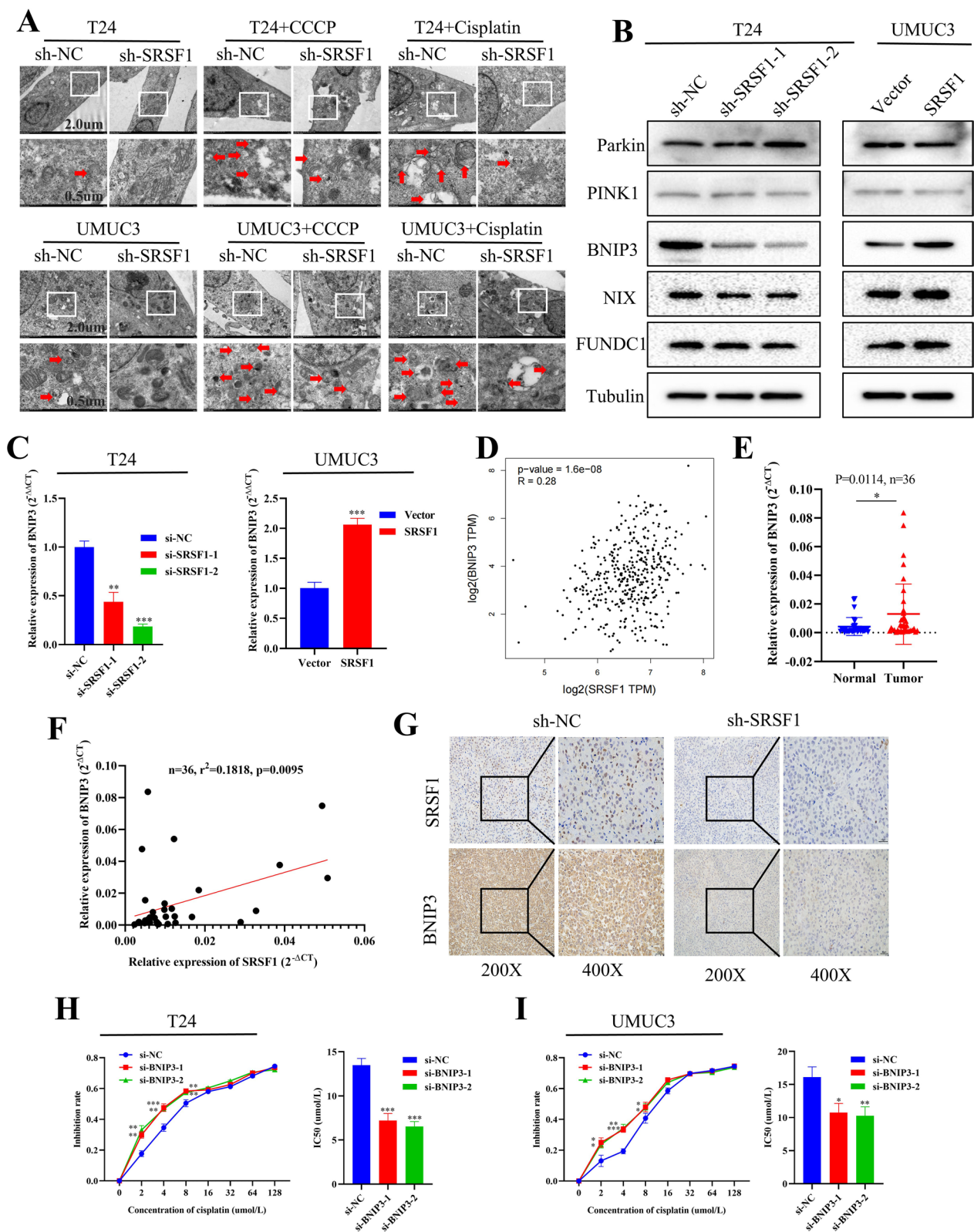


**Fig. 4** (See legend on previous page.)



with different SRSF1 fragments tagged with flag were constructed and transfected (Fig. 5J–K). Subsequent RIP analysis revealed that pre-HIF1A predominantly bound to the RRM1 and RRM2 regions of SRSF1 (Fig. 5L). Collectively, these results demonstrated that SRSF1 facilitated AS by directly interacting with HIF1A.

#### HIF1A upregulated BNIP3 expression by binding directly to the promoter region of BNIP3 in BCa Cells

Bioinformatics tools from Jasparr (<https://jaspar.elixir.no/>) predicted the HIF1A binding site within the BNIP3 promoter (Figs. 6A, S6A–B) and revealed potential sites around -495 to -490 bps and -131 to -126 bps from the transcription start site (Figs. 6B, S6C). Moreover, HIF1A's capability to bind the BNIP3 promoter had been validated using predictive modeling from the AlphaFold3 database (Fig. S6D). CUT & RUN analysis further confirmed significant enrichment of BNIP3 DNA with the predicted binding site during hypoxia through anti-HIF1A antibodies compared to anti-IgG (Fig. 6C). Pearson correlation analysis corroborated the positive association between HIF1A and BNIP3 expression (Fig. 6D). Luciferase reporter assays with wild-type (ACG TGC) and mutant (TGCACG) promoters in 293T cells under hypoxic conditions showed that mutations in the binding domain significantly inhibited transcriptional activation of the BNIP3 promoter (Fig. 6E–F). Western blotting analysis under hypoxic conditions revealed that interference with HIF1A significantly reduced BNIP3 expression (Fig. S6E–F); furthermore, when HIF1A was inhibited, this intervention also countered the SRSF1-induced increase in BNIP3 protein levels observed in T24 and UMUC3 cells (Fig. 6G–H).

#### BNIP3 knockdown rescued the SRSF1-promoted proliferation, migration and cisplatin-resistance of BCa cells through mitophagy pathway

To elucidate the role of SRSF1 in impeding the growth of BCa cells and mitigating cisplatin resistance via its regulatory effect on BNIP3, we selected si-BNIP3-2 based on

its superior knockdown efficiency for subsequent rescue experiments (Fig. S4). We transfected either si-BNIP3 or si-NC into SRSF1-overexpressing T24 and UMUC3 cells. Western blotting analysis revealed that the upregulation of BNIP3, mediated by SRSF1, was partially reversed following BNIP3 knockdown (Fig. 7A). The suppression of BNIP3 substantially reinstated the proliferative capabilities of T24 and UMUC3 cells, as evidenced by colony formation assays (Fig. 7B), CCK-8 assays (Fig. 7C), and EdU assays (Fig. 7D). Additionally, the knockdown of BNIP3 mitigated the SRSF1-induced increase in the migration rates of T24 and UMUC3 cells, as observed in scratch wound healing and transwell assays (Fig. S7). This BNIP3 suppression notably diminished the inhibition rate of cisplatin induced by SRSF1 overexpression. Furthermore, the concurrent BNIP3 knockdown counteracted the reduced cisplatin sensitivity and elevated IC50 values facilitated by SRSF1 (Fig. 7E). To substantiate that the observed phenotypic changes related to mitophagy were governed by the aberrant regulation of the SRSF1-BNIP3 axis under cisplatin treatment, we conducted a series of rescue experiments in cisplatin-treated BCa cells. The mitophagy flux notably activated by SRSF1 was inhibited by BNIP3 interference after transfection with mRFP-GFP-LC3 adenovirus (Fig. 7F). Western blotting analysis also indicated that the suppression of BNIP3 could revert the increased autophagy levels induced by SRSF1 overexpression (Fig. 7G). Furthermore, TEM revealed that the SRSF1-induced augmentation in mitophagosome numbers was reversible upon the interference of BNIP3 (Figs. 7H, S3D–E). Taken together, in the presence of cisplatin, SRSF1-mediated mitophagy was promoted, thereby inhibiting cisplatin sensitivity in BCa cells.

#### Discussion

Cisplatin-based chemotherapy regimens are currently the first-line treatment for bladder cancer [26]. Although cisplatin demonstrates efficacy in certain instances, its overall sensitivity among BCa patients remains relatively low

(See figure on next page.)

**Fig. 5** SRSF1 regulated the splicing of HIF1A in BCa cells. **A** RNA sequencing on SRSF1 knockdown and control cells identified 5 kinds of splicing events, including 64.19% skipped exons (SE), 12.66% mutually exclusive exons (MXE), 8.47% alternative 3' splice sites (A3SS), 8.31% retained introns (RI), 6.37% alternative 5' splice sites (A5SS). **B** The RIP assay confirmed that SRSF1 was not able to bind to the pre-mRNA of BNIP3. **C** RT-PCR demonstrated that SRSF1 could not contribute to the production of BNIP3 isoforms. **D** The RIP assay confirmed that SRSF1 was able to bind to the pre-mRNA of HIF1A (\*\* $P < 0.01$ , Student's t-test). **E** Correlation analysis confirmed a positive association between SRSF1 and HIF1A in the TCGA-BLCA cohort. **F** The expression of HIF1A in BCa tissues was validated by RT-qPCR (\*\* $P < 0.01$ , Student's t-test). **G** Pearson's correlation analysis was applied to confirm the correlation of SRSF1 and HIF1A. **H** Diagram of the splicing variants of HIF1A RNA and RT-PCR detection of exon 14 inclusion/exclusion (HIF1A-I means exon 14 inclusion). **I** AS of exon 14 and expression of HIF1A isoforms were examined by RT-PCR. **J** Schematic diagram of SRSF1 domains and construction of 3 SRSF1 mutants:  $\Delta$ RRM1 (deleted RRM1),  $\Delta$ RRM2 (deleted RRM2),  $\Delta$ RS (deleted RS). All mutants were flag tagged. **K** Western blotting of SRSF1 and its mutants using anti-flag tag antibody. **L** RIP assays were carried out by using flag antibodies to determine the region of SRSF1 that could bind to pre-HIF1A (\* $P < 0.05$ , \*\*\* $P < 0.001$ , Student's t-test)

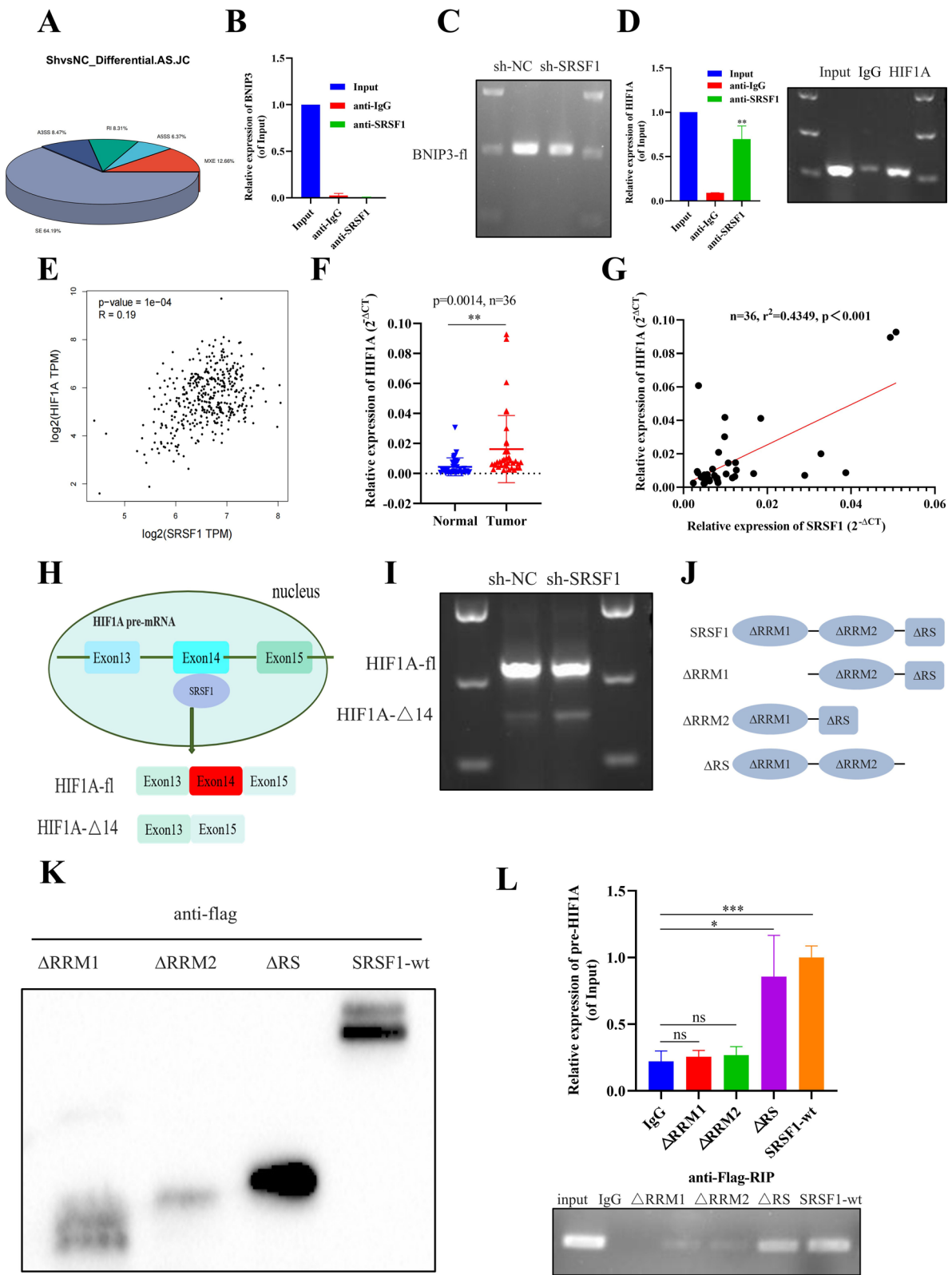


**Fig. 5** (See legend on previous page.)

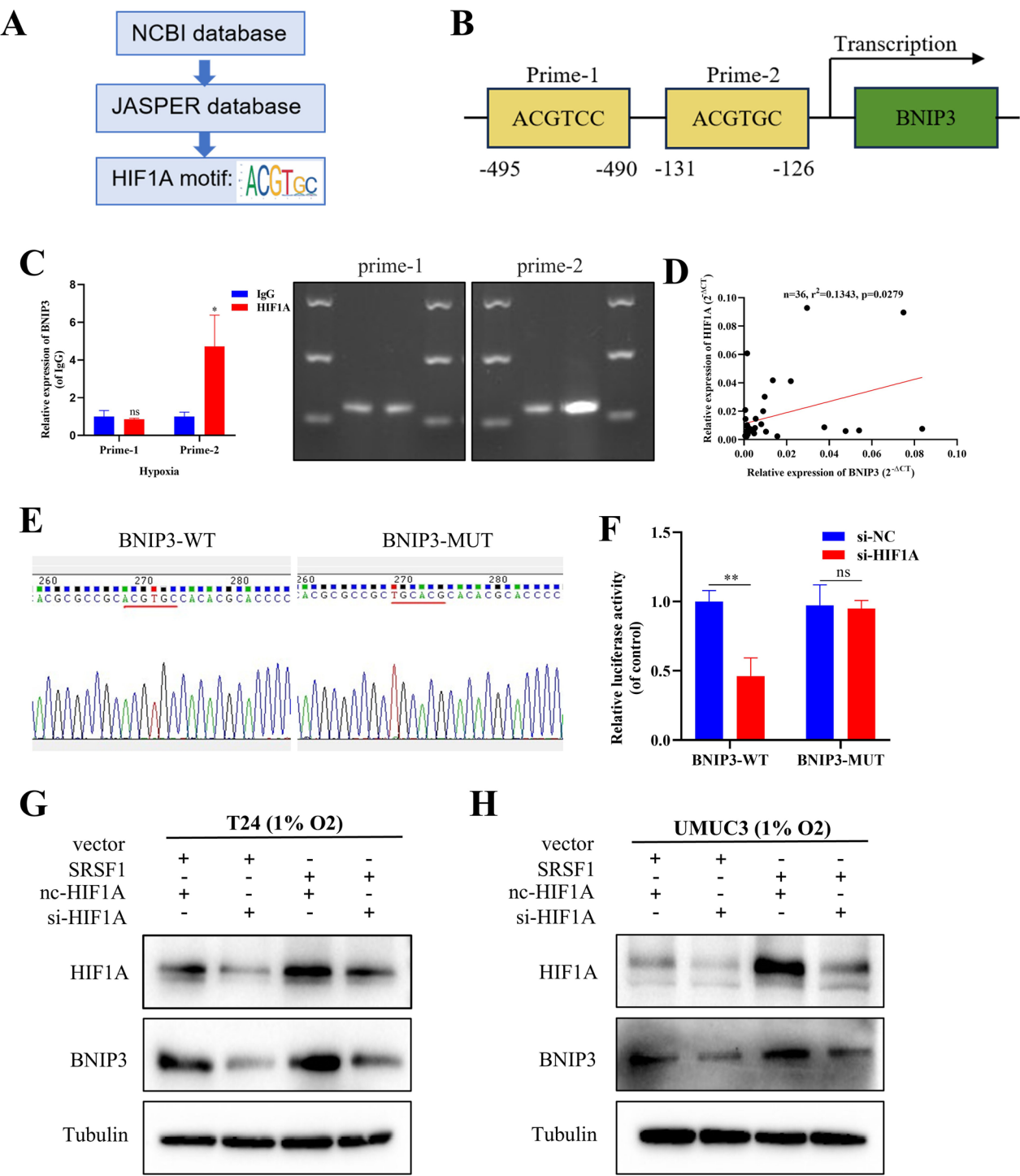


**Fig. 6** HIF1A upregulated BNIP3 expression by binding directly to the promoter region of BNIP3 in BCa Cells. **A–B** The predicted binding sites between HIF1A and BNIP3 promoter using Jaspas. **C** CUT & RUN analysis showed the significant enrichment of HIF1A in –131 to –126 bps of BNIP3 promoter in hypoxia (\* $P < 0.05$ , Student's t-test). **D** Pearson's correlation analysis was applied to confirm the correlation of BNIP3 and HIF1A. **E** Wild-type (ACGTGC) and mutant (TGCACG) luciferase reporters of the BNIP3 promoter region were constructed. **F** The relative activity of luciferase was measured in 293 T cells transfected with reporter plasmids containing fragments of the BNIP3 promoter. Then cells were exposed in hypoxia (1% O<sub>2</sub>) for 24 h. The ratio of firefly luciferase activity was determined and normalized against Renilla activity (\*\* $P < 0.01$ , Student's t-test). **G–H** Western blotting indicated that interfering with HIF1A during hypoxia could reverse the increased BNIP3 protein levels caused by overexpression of SRSF1

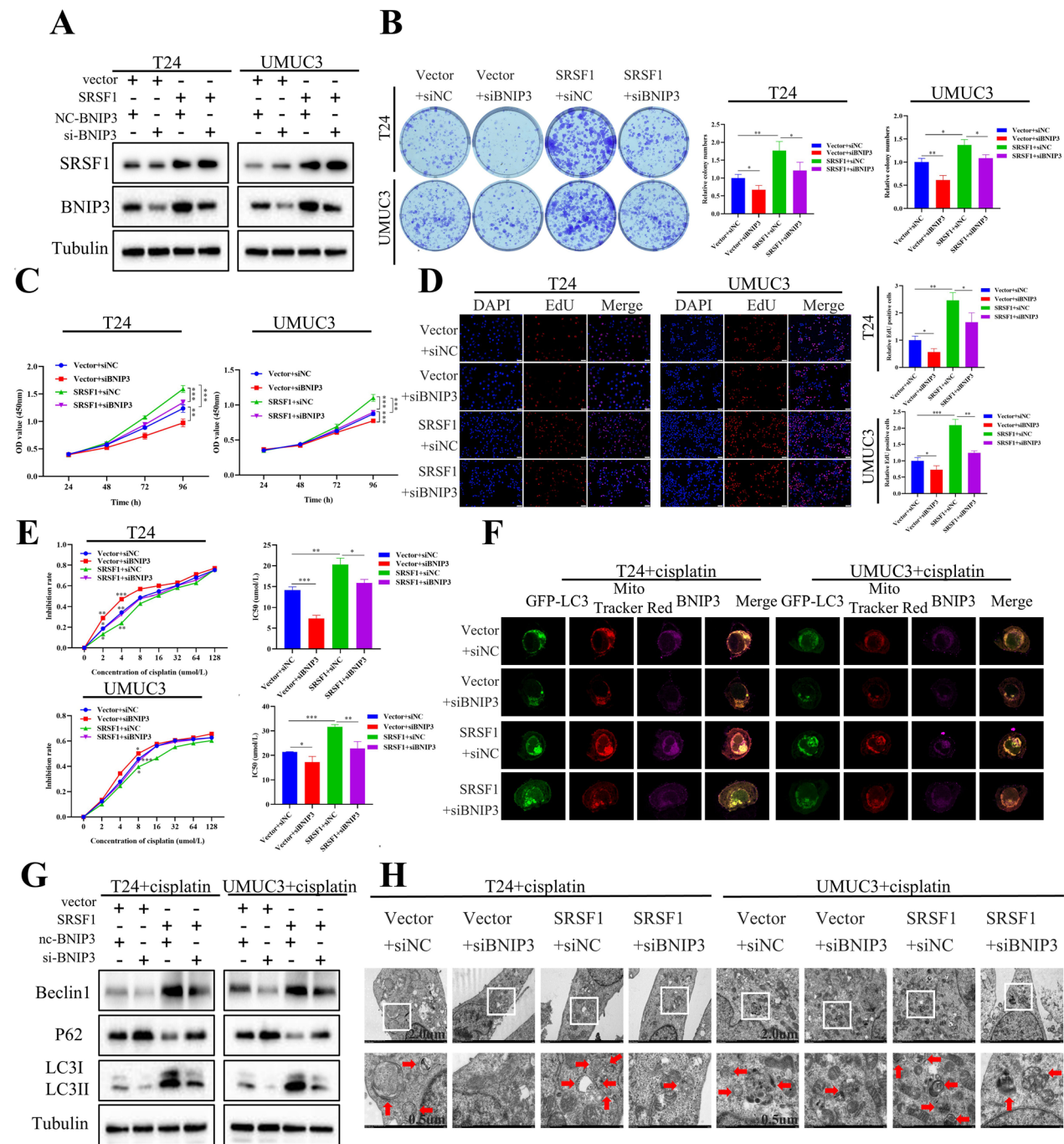


**Fig. 7** BNIP3 knockdown rescued the SRSF1-promoted proliferation, migration and cisplatin-resistance of BCa cells through mitophagy pathway. **A** Western blotting assays revealed that the knockdown of BNIP3 reversed the enhancement of BNIP3 induced by SRSF1 overexpression in T24 and UMUC3 cells. **B–D** The knockdown of BNIP3 significantly restored the proliferation of T24 and UMUC3 cells promoted by SRSF1 in colony formation assays, CCK-8 assays, and EdU assays ( $P < 0.05$ ,  $**P < 0.01$ ,  $***P < 0.001$ , Student's t-test). **E** The knockdown of BNIP3 could counteract the decreased cisplatin sensitivity and increased IC50 value induced by SRSF1 in T24 and UMUC3 cells ( $P < 0.05$ ,  $**P < 0.01$ ,  $***P < 0.001$ , Student's t-test). **F** The colocalization of mitochondria and autophagosomes demonstrated that mitophagy reflux activated by SRSF1 was also inhibited by the interference of BNIP3 under cisplatin conditions. **G** Western blotting results indicated that knocking down BNIP3 can reverse the increase of key proteins in autophagy levels caused by overexpression of SRSF1 under cisplatin conditions. **H** The transmission electron microscope analysis identified that SRSF1-induced increase in mitophagosome numbers could be reversed by interference with BNIP3 under cisplatin conditions



[27]. Despite extensive research efforts aimed at enhancing cisplatin sensitivity, the underlying mechanisms in bladder cancer are still not fully understood.

SRSF1, initially identified as SF2/ASF in the early 1990s, was characterized as an essential splicing factor for both constitutive and alternative pre-mRNA splicing [28]. Subsequently, studies have demonstrated that SRSF1 is involved in additional critical cellular processes, such as mRNA export, translation, and nonsense-mediated decay (NMD) [29–31]. Our current study indicates an upregulation of SRSF1 in BCa tissues and cell lines, with this overexpression correlating with poor prognosis and higher pathological grades. Presently, there is a paucity of reports regarding the direct role of SRSF1 in the malignant phenotype and specific chemoresistance associated with BCa. This suggests that SRSF1 could potentially serve as a prognostic marker for bladder cancer.

Previous research has elucidated the role of SRSF1 in the progression of various cancers, such as hepatocellular carcinoma [32], lung cancer [33], and osteosarcoma [34]. Results from our current study demonstrate that the downregulation of SRSF1 leads to decreased cell proliferation and migration, as well as enhanced sensitivity to cisplatin in T24 and UMUC3 cells. In contrast, overexpression of SRSF1 shows opposing effects. Complementary *in vivo* investigations reveal that silencing SRSF1 in T24 cells substantially decreases tumor volume and augments cisplatin sensitivity in nude mice. These findings suggest a contributory role for SRSF1 in both the advancement of BCa and the development of resistance to cisplatin. To investigate the mechanism of SRSF1 in BCa, further transcriptome sequencing was conducted.

RNA sequencing analysis revealed significant enrichment in the mitophagy pathway following the knockdown of SRSF1. Prior studies have indicated that autophagy facilitates the proliferation [35, 36] and chemoresistance to cisplatin [37, 38] of BCa cells. In our prior research, autophagy was shown to protect BCa cells and reduce drug sensitivity under the harsh conditions of chemotherapy [39]. Mitophagy, a specialized form of autophagy, selectively targets and degrades damaged mitochondria, preventing the accumulation of dysfunctional mitochondria and aiding in sustaining cellular homeostasis [16]. Various findings support that mitophagy propels tumor progression and augments cisplatin resistance [23, 40, 41]. Studies like those by Song et al. [42], which showed that lncRNA-RP11-498C9.13 might enhance bladder cancer tumorigenesis via ROS-induced mitophagy, and Sun et al. [43], which identified that METTL3-induced mitophagy contributes to chemoresistance in small cell lung cancer, align with our *in vitro* and *in vivo* outcomes. In profiling SRSF1's downstream targets, BNIP3 emerged as significantly regulated

in both the overexpression and knockdown contexts of SRSF1 due to its notable transcriptional changes. Further validation by western blotting of two mitophagy pathways corroborated the consistent modifications in BNIP3, NIX, and FUNDC1 within the ubiquitin-independent pathway, with BNIP3 showing the most pronounced changes. BNIP3, a crucial component of the ubiquitin-independent mitophagy pathway, has been extensively researched. Lin et al. [44] highlighted for its role in protecting against cisplatin-induced ferroptosis in renal tubular epithelial cells via mitophagy mediation. Additional research indicates that BNIP3-mediated mitochondrial clearance is vital for conferring cisplatin resistance, where the absence of BNIP3 resensitizes resistant cells to cisplatin by altering mitochondrial autophagy levels [22]. Consequently, we conclude that BNIP3 could potentially serve as a crucial target for SRSF1 in controlling the malignant phenotype of BCa. BCa cells with SRSF1 knockdown showed downregulated BNIP3, linked with reduced mitophagy rates and increased cisplatin sensitivity, emphasizing SRSF1's potential involvement in the ubiquitin-independent mitophagy pathway. Our findings also show that cisplatin, similar to CCCP, can induce mitophagy, aligning with studies that have reported mitochondrial damage-induced mitophagy by cisplatin [45]. Considering mitochondria as tumor cells' energy sources, the role of mitophagy in promoting malignant tumor phenotypes is increasingly evident [7]. This highlights the potential of targeting BNIP3 and mitophagy to enhance sensitization in traditional comprehensive therapy for bladder cancer.

Previous studies have focused primary attention on SRSF1 as an RNA splicing factor that drives tumor progression through alternative splicing mechanisms [46, 47]. Zhou et al. [14] demonstrated that the splicing of MYO1B by SRSF1 significantly enhanced proliferation and metastasis in glioma cells. Furthermore, SRSF1 was shown to promote the expression of the antiapoptotic splice isoform caspase 9b in lung cancer [48]. A recent study revealed that reduced levels of SRSF1 led to the production of shorter isoforms of PTPMT1, thus making cancer cells more susceptible to irradiation [49]. Additionally, evidence suggests that SRSF1 facilitates the splicing of MNK2b, thereby reducing the sensitivity of pancreatic ductal adenocarcinoma cells to chemotherapy, which is consistent with our research findings [15].

In our analysis of SRSF1-regulated AS events, we identified five distinct types of splicing events in the RNA sequencing data. SE events accounted for 64.19% of all events, confirming previous findings that SE events are predominant [13]. Consequently, our focus shifted to genes regulated by SE splicing among the validated SRSF1-affected AS events. Initially, it was hypothesized

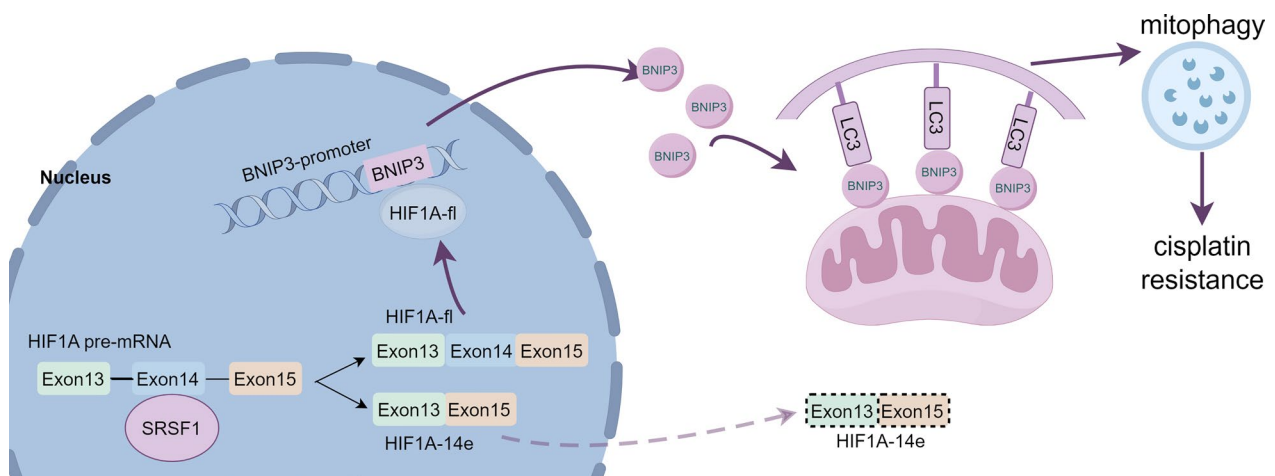


**Fig. 8** Mechanism pattern of the SRSF1/HIF1A/BNIP3 regulatory and function network

that SRSF1 could potentially bind to BNIP3 pre-mRNA. However, subsequent experiments involving RIP and RT-PCR disproved this hypothesis. Subsequently, we discovered that BNIP3 is a target gene of the transcription factor HIF1A in the mitophagy pathway. We demonstrated the generation of HIF1A alternative splicing isoforms by RT-PCR experiments using AS primers, which corroborated the findings reported by Daniel et al. [50]. Analysis of AS events in the transcriptome revealed that exon 14 of HIF1A is subject to alternative splicing. Observations indicated that SRSF1 knockdown significantly induced the skipping of exon 14, thereby promoting the expression of a truncated HIF1A isoform in knockdown cells. Meanwhile, RIP experiments further confirmed that SRSF1 binds through its RRM1/RRM2 structural domains, rather than RS to pre-HIF1A, which perfected the mechanism of SRSF1 in alternative splicing in bladder cancer cells. Therefore, we concluded that SRSF1 has the potential to indirectly induce BNIP3 production through the splicing of HIF1A. To further substantiate the hypothesis that SRSF1 modulates the sensitivity of bladder cancer cells to cisplatin through the HIF1A/BNIP3/mitophagy pathway, we employed both CUT&RUN and luciferase reporter assays. The implementation of these methods confirmed that HIF1A binds to the promoter region of BNIP3, further promoting transcriptional activation.

In our research, we have established that SRSF1 enhances mitophagy by supporting the alternative splicing of HIF1A and subsequent upregulation of BNIP3. This mechanism significantly enhances the survival and

proliferation of BCa cells under cisplatin-based chemotherapy. The current study is limited by its sample size. Data from cisplatin-sensitive and insensitive patients is being categorized and collected. Explorations into the combination of SRSF1 inhibitors and mitochondrial autophagy inhibitors are planned for the subsequent phase of chemotherapy for sensitized bladder cancer.

## Conclusion

SRSF1 is recognized as a crucial regulator of mitophagy in bladder cancer, promoting tumor progression and increasing resistance to chemotherapy via the HIF1A/BNIP3 pathway. Our research provides substantial insights into the essential role of SRSF1 in the pathophysiology of BCa and highlights its potential as a therapeutic target. Targeting this pathway could potentially enhance treatment outcomes for BCa patients. The mechanistic network involving SRSF1 is detailed in Fig. 8.

## Abbreviations

BCa	Bladder cancer
SRSF1	Serine-rich/arginine splicing factor 1
RT-qPCR	Quantitative real-time PCR
CCK-8	Cell counting kit-8
RIP	RNA immunoprecipitation
HIF1A	Hypoxia-inducible factor 1 alpha
BNIP3	BCL2-interacting protein 3
CUT & RUN	Cleavage Under Targets & Release Using Nuclease
JC-1	Mitochondrial membrane potential detection kit
MMP	Mitochondrial membrane potential
AS	Alternative splicing
SE	Skipped exon
CCCP	Carbonyl cyanide 3-chlorophenylhydrazone
EdU	5-Ethynyl-2'-deoxyuridine
IC50	Half maximal inhibitory concentration
TEM	Transmission electron microscopy

## Supplementary Information

The online version contains supplementary material available at <https://doi.org/10.1186/s12967-025-06547-7>.

Additional file 1. Figure S1: SRSF1 promoted the migration of BCa cells. **A–B** Transwell assays showed that SRSF1 knockdown could inhibit the migration rate while SRSF1 overexpression could promote the migration rate of T24 and UMUC3 cells. (\*\* $P < 0.01$ , Student's t-test). **C–D** Scratch wound healing assays showed that SRSF1 knockdown could inhibit the migration rate while SRSF1 overexpression could promote the migration rate of T24 and UMUC3 cells (\*\* $P < 0.01$ , Student's t-test)

Additional file 2. Figure S2: The efficiency of SRSF1 knockdown and screening of downstream targets of SRSF1 in BCa cells. **A** SRSF1 knockdown efficiency in T24 and UMUC3 cells was confirmed by RT-qPCR. (\*\*\* $P < 0.001$ , Student's t-test). **B** SRSF1 knockdown efficiency in T24 and UMUC3 cells was confirmed by western blotting. **C–D** The mito-Keima system for monitoring mitophagy. By transfecting mito-Keima plasmid into T24 or UMUC3 cells, we can observe the mitochondrial network (green signal) and mitochondria within acidic autolysosomes (red puncta). After adding CCCP or cisplatin, the number of red puncta increases. **E–F** RT-qPCR assay demonstrated downstream target BNIP3 in the mitophagy pathway was significantly altered with SRSF1 knockdown or overexpression compared with other potential targets (\* $P < 0.05$ , \*\* $P < 0.01$ , \*\*\* $P < 0.001$ , Student's t-test)

Additional file 3. Figure S3: The statistical analysis of changes in the number of mitophagosomes from TEM assays and the protein expression of BNIP3 in BCa tissue. **A–B** The number of mitophagosomes was reduced in SRSF1 knockdown cells compared to the negative control group. Treatment with CCCP or cisplatin increased mitophagosomes production in T24 and UMUC3 cells (\* $P < 0.05$ , \*\* $P < 0.01$ , Student's t-test). **C** The expression of BNIP3 in 8 pairs of BCa tissues was validated by western blotting. **D–E** Analysis of mitophagosome numbers revealed that the SRSF1-induced increase in mitophagosome count could be reversed by BNIP3 interference under cisplatin treatment (\* $P < 0.05$ , \*\* $P < 0.01$ , Student's t-test)

Additional file 4. Figure S4: BNIP3 promoted the proliferation and migration of BCa cells. **A–B** BNIP3 knockdown efficiency in T24 and UMUC3 cells was confirmed by RT-qPCR and western blotting (\*\* $P < 0.01$ , \*\*\* $P < 0.001$ , Student's t-test). **C–F** BNIP3 knockdown could inhibit the proliferation of T24 and UMUC3 cells through CCK8 assay, colony formation assay, and EdU assay (\* $P < 0.05$ , \*\* $P < 0.01$ , \*\*\* $P < 0.001$ , Student's t-test). **G–J** BNIP3 knockdown could inhibit the migration rate of T24 and UMUC3 cells through transwell assays and scratch wound assays (\* $P < 0.05$ , \*\* $P < 0.01$ , \*\*\* $P < 0.001$ , Student's t-test)

Additional file 5. Figure S5: SRSF1 regulated the splicing of HIF1A in cells. **A** HIF1A was upstream of BNIP3 in the mitophagy pathway in the RNA sequencing. **B** The splicing site of exon 14 skips of HIF1A in RNA sequencing

Additional file 6. Figure S6: HIF1A bound to the promoter region of BNIP3 in BCa Cells. **A** The JaspAr predicted several binding sites between the HIF1A and BNIP3 promoters. **B** The predicted binding motif between HIF1A and BNIP3 promoter regions. **C** The binding sites of HIF1A on BNIP3 predicted by Jasper database were labeled in yellow. **D** HIF1A could bind to the promoter of BNIP3 in the AlphaFold3 database. **E–F** Western blotting analysis indicated that interfering with HIF1A during hypoxia decreased the levels of the BNIP3 protein

Additional file 7. Figure S7: BNIP3 rescued the SRSF1-promoted migration and proliferation of BCa cells. **A–B** The knockdown of BNIP3 significantly restored the migration rates of T24 and UMUC3 cells promoted by SRSF1 by transwell assays (\* $P < 0.05$ , \*\* $P < 0.01$ , Student's t-test). **C–D** The knockdown of BNIP3 significantly restored the migration rates of T24 and UMUC3 cells promoted by SRSF1 by scratch wound assays (\* $P < 0.05$ , \*\*\* $P < 0.001$ , Student's t-test)

Additional file8 (DOCX 16 KB)

Additional file9 (DOCX 17 KB)

## Acknowledgements

Not applicable.

## Author contributions

QKW and HY drafted the article and interpreted data. QKW, JTZ, KXB, LLJ and YHC performed the experiments and obtained the data. JCL and HYS conducted bioinformatic analysis. LKC and YRT collected clinical samples and followed up patients' information. QL, XY, and HWY designed the study and revised the article critically for important intellectual content. All authors read and approved the final manuscript.

## Funding

National Natural Science Foundation of China (grants No. 82273152); Noncommunicable Chronic Diseases-National Science and Technology Major Project (2024ZD0525700); Jiangsu Province Hospital (the First Affiliated Hospital of Nanjing Medical University) Clinical Capacity Enhancement Project (JSPH-MA-2022–5); Natural Science Foundation of Jiangsu Province (grants No. BK20241128); China Postdoctoral Science Foundation (grants No. 2024M761211); Nanjing Postdoctoral Science Foundation funded project (grants No. 2024BHS210); and Jiangsu Funding Program for Excellent Postdoctoral Talent.

## Availability of data and materials

The datasets supporting the conclusions of this article are included within the article and its supplementary files.

## Declarations

### Ethics approval and consent to participate

The Ethics Committee of The First Affiliated Hospital of Nanjing Medical University approved all human-associated tissues used in this research. The informed consent has been signed by all patients before their tissues were acquired.

### Consent for publication

Not applicable.

### Competing interests

The authors declare that they have no conflict of interest.

### Author details

<sup>1</sup>Department of Urology, The First Affiliated Hospital of Nanjing Medical University, Nanjing 210029, China. <sup>2</sup>Laboratory of Urology and Andrology, Jiangsu Clinical Medicine Research Institution, Nanjing 210029, China. <sup>3</sup>Department of Urology, First Affiliated Hospital, School of Medicine, Zhejiang University, Hangzhou 310058, China.

Received: 23 October 2024 Accepted: 29 April 2025

Published online: 22 May 2025

## References

- Bray F, Laversanne M, Sung H, et al. Global cancer statistics 2022: GLOBOCAN estimates of incidence and mortality worldwide for 36 cancers in 185 countries. *CA Cancer J Clin*. 2022;74(2024):229–63.
- Lenis AT, Lec PM, Chamie K, et al. Bladder cancer: a review. *JAMA*. 2020;324:1980–91.
- Pfister C, Gravis G, Flechon A, et al. Perioperative dose-dense methotrexate, vinblastine, doxorubicin, and cisplatin in muscle-invasive bladder cancer (VESPER): survival endpoints at 5 years in an open-label, randomised, phase 3 study. *Lancet Oncol*. 2024;25:255–64.
- Pfister C, Gravis G, Flechon A, et al. Randomized phase III trial of dose-dense methotrexate, vinblastine, doxorubicin, and cisplatin, or gemcitabine and cisplatin as perioperative chemotherapy for patients with muscle-invasive bladder cancer. Analysis of the GETUG/AFU V05 VESPER trial secondary endpoints: chemotherapy toxicity and pathological responses. *Eur Urol*. 2021;79:214–21.



5. Liu M, Zhang S, Zhou H, et al. The interplay between non-coding RNAs and alternative splicing: from regulatory mechanism to therapeutic implications in cancer. *Theranostics*. 2023;13:2616–31.
6. Dvinge H, Kim E, Abdel-Wahab O, et al. RNA splicing factors as oncoproteins and tumour suppressors. *Nat Rev Cancer*. 2016;16:413–30.
7. Zheng X, Peng Q, Wang L, et al. Serine/arginine-rich splicing factors: the bridge linking alternative splicing and cancer. *Int J Biol Sci*. 2020;16:2442–53.
8. Paz S, Ritchie A, Mauer C, et al. The RNA binding protein SRSF1 is a master switch of gene expression and regulation in the immune system. *Cytokine Growth Factor Rev*. 2021;57:19–26.
9. Das S, Krainer AR. Emerging functions of SRSF1, splicing factor and oncoprotein, RNA metabolism and cancer. *Mol Cancer Res*. 2014;12:1195–204.
10. Das S, Anczukow O, Akerman M, et al. Oncogenic splicing factor SRSF1 is a critical transcriptional target of MYC. *Cell Rep*. 2012;1:110–7.
11. Arif W, Mathur B, Saikali MF, et al. Splicing factor SRSF1 deficiency in the liver triggers NASH-like pathology and cell death. *Nat Commun*. 2023;14:551.
12. Zhao J, Jiang Y, Zhang H, et al. The SRSF1/circATP5B/miR-185-5p/HOXB5 feedback loop regulates the proliferation of glioma stem cells via the IL6-mediated JAK2/STAT3 signaling pathway. *J Exp Clin Cancer Res*. 2021;40:134.
13. Du JX, Luo YH, Zhang SJ, et al. Splicing factor SRSF1 promotes breast cancer progression via oncogenic splice switching of PTPMT1. *J Exp Clin Cancer Res*. 2021;40:171.
14. Zhou X, Wang R, Li X, et al. Splicing factor SRSF1 promotes gliomagenesis via oncogenic splice-switching of MYO1B. *J Clin Invest*. 2019;129:676–93.
15. Adesso L, Calabretta S, Barbagallo F, et al. Gemcitabine triggers a pro-survival response in pancreatic cancer cells through activation of the MNK2/eIF4E pathway. *Oncogene*. 2013;32:2848–57.
16. Song C, Pan S, Zhang J, et al. Mitophagy: a novel perspective for insight into cancer and cancer treatment. *Cell Prolif*. 2022;55:e13327.
17. Zhang T, Liu Q, Gao W, et al. The multifaceted regulation of mitophagy by endogenous metabolites. *Autophagy*. 2022;18:1216–39.
18. Wu X, Zheng Y, Liu M, et al. BNIP3L/NIX degradation leads to mitophagy deficiency in ischemic brains. *Autophagy*. 2021;17:1934–46.
19. Hui L, Wu H, Wang TW, et al. Hydrogen peroxide-induced mitophagy contributes to laryngeal cancer cells survival via the upregulation of FUNDC1. *Clin Transl Oncol*. 2019;21:596–606.
20. Zhao C, Chen Z, Qi J, et al. Drp1-dependent mitophagy protects against cisplatin-induced apoptosis of renal tubular epithelial cells by improving mitochondrial function. *Oncotarget*. 2017;8:20988–1000.
21. Chen L, Yao Y, Sun L, et al. Galectin-1 promotes tumor progression via NF- $\kappa$ B signaling pathway in epithelial ovarian cancer. *J Cancer*. 2017;8:3733–41.
22. Vianello C, Cocetta V, Catanzaro D, et al. Cisplatin resistance can be curtailed by blunting Bnip3-mediated mitochondrial autophagy. *Cell Death Dis*. 2022;13:398.
23. Yan C, Luo L, Guo CY, et al. Doxorubicin-induced mitophagy contributes to drug resistance in cancer stem cells from HCT8 human colorectal cancer cells. *Cancer Lett*. 2017;388:34–42.
24. Hou H, Er P, Cheng J, et al. High expression of FUNDC1 predicts poor prognostic outcomes and is a promising target to improve chemoradiotherapy effects in patients with cervical cancer. *Cancer Med*. 2017;6:1871–81.
25. Abdakhmanov A, Kulikov AV, Luchkina EA, et al. Involvement of mitophagy in cisplatin-induced cell death regulation. *Biol Chem*. 2019;400:161–70.
26. Kool R, Dragomir A, Kulkarni GS, et al. Benefit of neoadjuvant cisplatin-based chemotherapy for invasive bladder cancer patients treated with radiation-based therapy in a real-world setting: an inverse probability treatment weighted analysis. *Eur Urol Oncol*. 2024.
27. Sjobahl G, Abrahamsson J, Holmsten K, et al. Different responses to neoadjuvant chemotherapy in urothelial carcinoma molecular subtypes. *Eur Urol*. 2022;81:523–32.
28. Krainer AR, Conway GC, Kozak D. The essential pre-mRNA splicing factor SF2 influences 5' splice site selection by activating proximal sites. *Cell*. 1990;62:35–42.
29. Jin X. Regulatory network of serine/arginine-rich (SR) proteins: the molecular mechanism and physiological function in plants. *Int J Mol Sci*. 2022;23.
30. Scott HM, Smith MH, Coleman AK, et al. Serine/arginine-rich splicing factor 7 promotes the type I interferon response by activating Irf7 transcription. *Cell Rep*. 2024;43:113816.
31. Leclair NK, Brugiolo M, Urbanski L, et al. Poison exon splicing regulates a coordinated network of sr protein expression during differentiation and tumorigenesis. *Mol Cell*. 2020;80:648–665 e649.
32. Wu Y, Wang J, Zhao J, et al. LTR retrotransposon-derived LncRNA LINC01446 promotes hepatocellular carcinoma progression and angiogenesis by regulating the SRPK2/SRSF1/VEGF axis. *Cancer Lett*. 2024;598:217088.
33. Mao S, Wu D, Cheng X, et al. Circ\_0007432 promotes non-small cell lung cancer progression and macrophage M2 polarization through SRSF1/KLF12 axis. *iScience*. 2024;27:109861.
34. Li S, Huang X, Zheng S, et al. High expression of SRSF1 facilitates osteosarcoma progression and unveils its potential mechanisms. *BMC Cancer*. 2024;24:580.
35. Hwang TI, Chen PC, Tsai TF, et al. Hsa-miR-30a-3p overcomes the acquired protective autophagy of bladder cancer in chemotherapy and suppresses tumor growth and muscle invasion. *Cell Death Dis*. 2022;13:390.
36. Lin YC, Lin JF, Wen SJ, et al. Inhibition of high basal level of autophagy induces apoptosis in human bladder cancer cells. *J Urol*. 2016;195:1126–35.
37. Mao X, Nanzhang, Xiao J, et al. Hypoxia-induced autophagy enhances cisplatin resistance in human bladder cancer cells by targeting hypoxia-inducible factor-1 $\alpha$ . *J Immunol Res*. 2021;2021:8887437.
38. Fan Z, Huangfu X, Liu Z. Effect of autophagy on cisplatin-induced bladder cancer cell apoptosis. *Panminerva Med*. 2017;59:1–8.
39. Yu H, Zhuang J, Zhou Z, et al. METTL16 suppressed the proliferation and cisplatin-chemoresistance of bladder cancer by degrading PMEPA1 mRNA in a m6A manner through autophagy pathway. *Int J Biol Sci*. 2024;20:1471–91.
40. Mukherjee S, Bhatti GK, Chhabra R, et al. Targeting mitochondria as a potential therapeutic strategy against chemoresistance in cancer. *Biomed Pharmacother*. 2023;160:114398.
41. Liu L, Zuo Z, Lu S, et al. Silencing of PINK1 represses cell growth, migration and induces apoptosis of lung cancer cells. *Biomed Pharmacother*. 2018;106:333–41.
42. Song W, Li Z, Yang K, et al. Antisense lncRNA-RP11-498C9.13 promotes bladder cancer progression by enhancing reactive oxygen species-induced mitophagy. *J Gene Med*. 2023;25:e3527.
43. Sun Y, Shen W, Hu S, et al. METTL3 promotes chemoresistance in small cell lung cancer by inducing mitophagy. *J Exp Clin Cancer Res*. 2023;42:65.
44. Lin Q, Li S, Jin H, et al. Mitophagy alleviates cisplatin-induced renal tubular epithelial cell ferroptosis through ROS/HO-1/GPX4 axis. *Int J Biol Sci*. 2023;19:1192–210.
45. Lu H, Tong W, Jiang M, et al. Mitochondria-targeted multifunctional nanoprodrugs by inhibiting metabolic reprogramming for combating cisplatin-resistant lung cancer. *ACS Nano*. 2024;18:21156–70.
46. Li WJ, Huang Y, Lin YA, et al. Targeting PRMT1-mediated SRSF1 methylation to suppress oncogenic exon inclusion events and breast tumorigenesis. *Cell Rep*. 2023;42:113385.
47. Wan L, Lin KT, Rahman MA, et al. Splicing factor SRSF1 promotes pancreatitis and KRASG12D-mediated pancreatic cancer. *Cancer Discov*. 2023;13:1678–95.
48. Shultz JC, Goehe RW, Murudkar CS, et al. SRSF1 regulates the alternative splicing of caspase 9 via a novel intronic splicing enhancer affecting the chemotherapeutic sensitivity of non-small cell lung cancer cells. *Mol Cancer Res*. 2011;9:889–900.
49. Sheng J, Zhao Q, Zhao J, et al. SRSF1 modulates PTPMT1 alternative splicing to regulate lung cancer cell radioresistance. *EBioMedicine*. 2018;38:113–26.
50. Comiskey DF Jr, Jacob AG, Singh RK, et al. Splicing factor SRSF1 negatively regulates alternative splicing of MDM2 under damage. *Nucleic Acids Res*. 2015;43:4202–18.

## Publisher's Note

Springer Nature remains neutral with regard to jurisdictional claims in published maps and institutional affiliations.